HHS Public Access

Author manuscript

Mol Cancer Ther. Author manuscript; available in PMC 2016 May 01.

Published in final edited form as:

Mol Cancer Ther. 2015 May ; 14(5): 1247–1258. doi:10.1158/1535-7163.MCT-14-0913.

Enhancement of the pro-apoptotic properties of Newcastle disease virus promotes tumor remission in syngeneic murine cancer models

Sara Cuadrado-Castano[1,2], **Juan Ayllon**[2,6], **Mena Mansour**[3], **Janis de la Iglesia-Vicente**[3], **Stefan Jordan**[4], **Shashank Tripathi**[2], **Adolfo García-Sastre**[2,5,6], and **Enrique Villar**[1]

[1]Department of Biochemistry and Molecular Biology, University of Salamanca, Salamanca, Spain

[2]Department of Microbiology, Icahn School of Medicine at Mount Sinai, New York, New York, USA

[3]Department of Pathology, Icahn School of Medicine at Mount Sinai, New York, New York, USA

[4]Department of Oncological Sciences, Immunology Institute and the Tisch Cancer Institute, Icahn School of Medicine at Mount Sinai, New York, New York, USA

[5]Department of Medicine, Division of Infectious Disease, Icahn School of Medicine at Mount Sinai, New York, New York, USA

[6]Global Health and Emerging Pathogens Institute, Icahn School of Medicine at Mount Sinai, New York, New York, USA

Abstract

Newcastle disease virus (NDV) is considered a promising agent for cancer therapy due to its oncolytic properties. These include preferential replication in transformed cells, induction of innate and adaptive immune responses within tumors and cytopathic effects in infected tumor cells due to the activation of apoptosis. In order to enhance the latter and thus possibly enhance the overall oncolytic activity of NDV, we generated a recombinant NDV encoding the human TNF receptor Fas (rNDV-B1/Fas). rNDV-B1/Fas replicates to similar titers as its wild type (rNDV-B1) counterpart, however overexpression of Fas in infected cells leads to higher levels of cytotoxicity correlated with faster and increased apoptosis responses in which both the intrinsic and extrinsic pathways are activated earlier. Furthermore, *in vivo* studies in syngeneic murine melanoma model show an enhancement of the oncolytic properties of rNDV-B1/Fas, with major improvements in survival and tumor remission. Altogether, our data suggest that up-regulation of the pro-apoptotic function of NDV is a viable approach to enhance its anti-tumor properties, and adds to the currently known, rationally-based strategies to design optimized therapeutic viral vectors for the treatment of cancer.

Correspondence: Adolfo García-Sastre, Ph.D., Icahn School of Medicine at Mount Sinai, Microbiology. 1468 Madison Avenue, New York, NY 10029, United States. Telephone: 212-241-7769; Fax: 212-534-1684, Adolfo.Garcia-Sastre@mssm.edu.

Conflict of interest: Icahn School of Medicine at Mount Sinai owns patent positions for reverse genetics of Newcastle disease viruses.

Keywords

Fas; apoptosis; oncolytic; virotherapy; recombinant virus

Introduction

Newcastle disease virus (NDV) is a negative sense single-stranded RNA virus classified as an avian paramyxovirus in the Avulavirus genus of the Family Paramyxoviridae (1). In the absence of vaccination, NDV outbreaks in poultry can cause devastating economic losses. However, NDV infections in humans are infrequent, and only cause mild conjunctivitis. The anti-tumor potential of NDV was first described during the 1960's (2). Since then, its natural oncolytic capabilities have been demonstrated in different mammalian cancer cell lines, animal tumor models and clinical trials (3–5). NDV selectively replicates in cancer cells inducing cell death and stimulating innate and adaptive immune responses against tumor cells. Together with the lack of preexisting immunity in the general population, NDV is a suitable candidate to be used as an oncolytic therapeutic agent (6). As with many oncolytic viruses, the establishment of reverse genetics systems for NDV facilitated the development of new genetically modified recombinant NDV viruses with improved anti-tumor properties (7, 8). The principal strategy followed by most research groups including ours, has been focused on the enhancement of NDV immunostimulatory properties through the generation of recombinant NDV viruses that express cytokines (IL-2, IFN-γ, TNF-α), tumor associated antigens (TAAs) or tumor–specific antibodies (9–13). In our quest to design an optimized therapeutic NDV vector, here we focused our efforts on enhancing the cancer killing potential of NDV by increasing its potential for apoptosis activation.

Apoptosis is a highly regulated form of death that cells undergo after activation by different, but specific, external or internal stimulation (14). There are two main apoptosis pathways: the extrinsic or death receptor pathway and the intrinsic or mitochondrial pathway (15). Each pathway is executed in a caspase-dependent manner and both pathways communicate by cross signaling in such a way that molecules from one pathway can influence the other. Apoptosis resistance is a major hallmark of most, if not all, types of cancers due to defects in the apoptotic pathways (16, 17).

Indeed apoptosis resistance has recently been identified as a marker for resistance to chemotherapy and poor prognosis in cancer patients (18, 19). Nevertheless, the oncolytic activity of NDV has been shown to correlate with activation of the intrinsic or mitochondrial apoptosis pathway even in cancer cells resistant to apoptosis induction (20–23).

In this study we propose a novel approach to enhance the oncolytic properties of NDV. By generating a recombinant NDV that encodes the human Tumor Necrosis Factor Receptor Fas we hypothesized that we would enhance the apoptotic and antitumor properties of NDV (24). Fas is one of the most important and better characterized death receptors due to its role in homeostasis, elimination of pathogen-infected cells and activation of the immune response (25–29). The transduction of the Fas-dependent death signal initiates from binding of its ligand FasL that results in receptor-mediated apoptosis signaling complex formation, and caspase-8 activation (30–33). Fas-mediated cytotoxicity is not only restricted to the

activation of the extrinsic pathway, but is also required for CTL-mediated perforin-granzyme cytotoxicity (34). Defects in the Fas-FasL system have been documented in many tumor types as a major feature of malignant progression, tumor immune evasion, and resistance to cytostatic drug treatment (35, 36).

In our current study we evaluated the anti-tumor potential of a newly generated rNDV-B1/Fas virus. We postulated that by overexpressing Fas in NDV-infected cells we will introduce a strong extrinsic pro-apoptotic stimulus that will synergize for apoptosis induction with the intrinsic pathways activated by NDV infection, translating into an enhancement of its anti-tumor phenotype *in vivo*.

Materials and Methods

Cell lines, antibodies and other reagents

Vero (African green monkey kidney epithelial cells; ATCC Cat# CCL-81, 2014), B16-F10 (mouse skin melanoma cells; ATCC Cat# CRL-6475, 2013), HeLa cells (human cervical adenocarcinoma epithelial cells; ATCC Cat# CCL-2, 2012), NIH/3T3 (murine embryonic fibroblast; ATCC Cat# CRL-1658, 2014), HuH-7 (human hepatocarcinoma; genteelly provided by Dr. Matthew Evans research group, Department of Microbiology, Icahn School of Medicine at Mount Sinai, New York, NY, 2014) and A549 cells (human lung carcinoma; ATCC Cat# CCL-185, 2014) were maintained in DMEM medium supplemented with 10% FBS (fetal bovine serum), L-Glutamine (1% Glutamax-100X, Invitrogen) penicillin and streptomycin (DMEM 10% FBS P/S). CT26 cells (ATCC Cat# 2638, 2013) were maintained in RPMI-NaHCO3 5% medium supplemented with 10% fetal bovine serum, penicillin and streptomycin. C-33A cells (human cervical carcinoma epithelial cells; ATCC Cat# HTB-31, 2012) were maintained in EMEM medium supplemented with 10% FBS (fetal bovine serum) and 5% of penicillin and streptomycin (Gibco by Life Technologies, Thermo Scientific, Rockford, IL). A master cell-bank was created for each cell line after purchase and early-passage cells were thawed in every experimental step. Once in culture, cells were maintained not longer than two months to guarantee genotypic stability and were monitored by microscopy. As a specific feature of the HuH-7 cells, ability to support HCV replication was demonstrated by Matthew Evans group (37).

Cell lysates for SDS-Page were obtained using the ProteoJET Mammalian Cell Lysis reagent purchased from Fermentas (Thermo Scientific, Rockford, IL). ECL Western Blotting System and HRP conjugated-secondary antibodies were purchased from GE Healthcare (Buckinghampsire, UK). ECL Western Blotting Substrate (Thermo Scientific. Rockford, IL) was used for detection of HRP in immunoblots.

Polyclonal antibodies to human/Fas (C18C12), anti-caspase 3, anti-caspase 9 and anti-PARP, as well as monoclonal antibody to caspase 8 were purchased from Cell Signaling (Boston, MA). Monoclonal anti-β-Actin (AC–15) was purchased from Abcam (Cambridge, MA). Rabbit polyclonal serum to NDV was previously described (38). Monoclonal antibody to human APO-1/Fas was for Bender MedSystems (San Diego, CA). Monoclonal mouse anti-IgG Alexa Fluor® 568 and poyclonal rabbit anti-IgG Alexa Fluor® 488 were purchased from Invitrogen (Molecular Probes, Eugene, OR). Hoechst 33258 nuclear staining reagent

was purchased from Invitrogen (Molecular Probes, Eugene, OR). MTT (3-(4,5-dimethylthiazolyl-2)-2,5-diphenyltetrazolium bromide) reagent was purchased from Sigma (St Louis, MO).

Generation of recombinant NDV

Plasmid pNDV-B1, encoding the full-length antigenomic cDNA of Hitchner B1 lentogenic strain of NDV has been previously described (8). The ORF of human Fas receptor was amplified by PCR using specific primers including the required regulatory signals for its functional integration into the NDV genome and then cloned into the XbaI site between the P and M genes of pNDV-B1. Recombinant rNDV-B1/Fas was rescued using previously described techniques (8). Insert fidelity was evaluated by amplification of the Fas sequence by reverse transcription PCR and virus genomic RNA followed by sequencing. Viral stocks of rNDV-B1/Fas and rNDV-B1 were propagated in 9 days embryonated chicken eggs and purified from the allantoic fluid in a potassium tartrate gradient.

Fluorescence microscopy

For indirect immunofluorescence staining, cells seeded in 24-well standard plates or glass-bottomed 12-well plates were infected for 1h at an MOI of 1 PFU/cell, after which the inoculum was removed and replaced with 1 ml of DMEM 10% FBS P/S. At 20 hours post-infection cells were fixed with 2.5% paraformaldehyde for 15 minutes and blocked in PBS 1% BSA for 1h. Primary antibodies were incubated with the samples for 1h at room temperature.

Secondary antibodies (goat anti-mouse Alexa Fluor 568 or 633 or goat anti-rabbit Alexa Fluor 488; purchased from Invitrogen, USA) were used at a 1:1000 dilution for 45 minutes prior to imaging using an Olympus IX41 microscope or a Zeiss LSM 510 Meta confocal microscope.

Growth curves and titers

HeLa, Vero, A549, HuH-7, C-33A and B16-F10 cells monolayers in 6 well plates were infected with the virus suspension at an MOI of 0.01 PFU/cell in OPTIMEM-I. After 1 hour, the infection media was removed and the cells were incubated with 3 ml of DMEM with 0.3% bovine serum albumin and 1 μg of TPCK-treated trypsin/ml to allow the production of fusion-competent viruses. Supernatants were collected at 24, 36, 48 and 64 hours (72 hours in A549, HuH-7, C-33A and B16-F10) post-infection and titrated by immunofluorescence assay on Vero cells seeded on 96 well plates by using a polyclonal anti-NDV serum.

MTT cytotoxicity assay

HeLa, A549, HuH-7, C-33A and B16-F10 cells were cultured at a confluence of 50% in 24 well dishes and infected at an MOI of 1 PFU/cell. Infection media was removed 1h post infection and cells were incubated 24, 36 and 48 hours in 1 ml of supplemented DMEM (or EMEM for C-33A). At each time point, the media was aspirated and cells were subsequently incubated 1 hour 15 minutes with 300 μl of 2.5 mg/ml MTT solution at 37°C and under restricted light conditions. Subsequently, the MTT solution was aspirated and cells were

incubated with 500 μl of Isopropanol for 10 minutes in a shaker. The absorbance of each sample was recorded at 570 nm using a BioTek plate reader.

Annexin-V/Propidium Iodide flow cytometric analysis

Cells were plated in 35mm dishes and infected an MOI of 1 PFU/cell. Infection media was removed 1h post infection and cells were incubated 24 and 48 hours in supplemented DMEM. Apoptosis induction was determined using the Immunostep DY-634 Annexin-V Apoptosis Detection Kit (Immunostep; Salamanca, Spain), according to the manufacturer's instructions. Cell acquisition was made on a FACSCalibur flow cytometer (Becton Dickinson).

Data analysis was performed using CellQuest, from BD Biosciences (San Jose, CA), and FlowJo software (Tree Star, Ashland, OR).

Caspase activity assay

HeLa cells were plated into 96 well plates and infected at an MOI of 1 PFU/cell. One hour post infection, the media was replaced by conventional DMEM or DMEM supplemented with caspase-specific inhibitor at different final concentrations. For specific caspase-activity inhibition the reagents InSolution™ Caspase 8 or InSolution™ Caspase 9 (EMD Millipore, Ref 218840 and 218841, respectively) were used. At 24 hours post-infection, Caspase 8, 9 and 3 activity was quantified by Caspase-Glo 8, 9 or 3/7 assay systems (Promega, G8210, G8211 an G8090, respectively) following manufacture's instructions.

Interferon response assay

B16-F10 and NIH/373 cells monolayers in 6 well plates were infected with the virus suspension at an MOI of 1 PFU/cell in OPTIMEM-I. After 1 hour, the infection media was removed and the cells were incubated with 3 ml of DMEM. Total RNAs from cultured cells were isolated 8 hours post-infectio with a Qiagen RNeasy Minikit (Qiagen). Mean n-fold expression levels of cDNA from three individual biological samples, each measured in triplicate, were normalized to 18S rRNA levels and calibrated to mock-treated samples according to the $2^{-\Delta\Delta CT}$ method (39).

The primer sequences were as follows: for the murine gene IFN-β, the forward primer was5′CAGCTCCAAGAAAGGACGAAC-3′ and the reverse primer was 5′GGCAGTGTAACTCTTCTGCAT-3′. Murine IFIT1, the forward primer was 5'CTGAGATGTCACTTCACATGGAA-3' and the reverse was 5'GTGCATCCCCAATGGGTTCT-3'. Murine gene OAS1, the forward primer was 5'ATGGAGCACGGACTCAGGA-3' and the reverse was 5' TCACACACGACATTGACGGC-3'. Murine IRF7 gene, the forward primer was 5'GAGACTGGCTATTGGGGGAG-3' and the reverse primer was 5'GACCGAAATGCTTCCAGGG-3'.

The 18S forward primer was 5′-GTAACCCGTTGAACCCCATT-3′, and the 18S reverse primer was 5′-CCATCCAATCGGTAGTAGCG-3′.

Syngeneic melanoma tumor model

C57/BL6J female mice 4–6 weeks of age used in all our *in vivo* studies were purchased form Jackson Laboratory (Bar Harbord, ME).

A B16-F10 cells suspension (5×10^5 cells in 100 μl of PBS) was intradermally inoculated into the flank of the right posterior leg of each C57/BL6J mouse. After 10 days, the mice were treated by intratumoral injection of 50 μl of 5×10^6 PFU of the indicated recombinant NDV viruses or PBS. The intratumoral injections were administered every 24 hours for a total of three treatment doses. Tumor volume was monitored every 48 hours or every 24 hours when the last volume estimation was approaching the experimental endpoint of 1000 mm^3. Mice were humanely euthanized the day in which the volume exceeded the predefined endpoint. Tumor measurement was determined using a digital caliper and total volume was calculated using the formula: Tumor volume (V) = $L\times W^2$, where L, or tumor length, is the larger diameter, and W, or tumor width, is the smallest diameter.

Immunohistochemistry (IHC) and immunofluorescence staining of tumor samples

A suspension of B16-F10 cells (5×10^5 cells in 100 μl of PBS) was intradermally inoculated into the flank of the right posterior leg of C57/BL6J mice. After 10 days, one intratumoral injection of PBS or recombinant NDV virus suspension (5×10^6 PFU in 50 μl of PBS) was administrated. At 24 hours post-inoculation, the tumors were removed and preserved by formalin-fixation and paraffin embedding for immunohistochemistry (ICH) analysis.

IHC staining for active caspase 3 was performed on 5 μm-thick tumor sections. The slides were incubated in H2O2 solution for 15 minutes and antigen retrieval was performed by steam heating in 10 mM citrate buffer (pH 6.0) for 45 minutes.

After epitope recovery, the slides were then treated with 10% of normal goat serum for 60 minutes, followed by incubation with caspase 3 antibody (1:500 dilution, Cell Signaling ref. 9664) incubation overnight at 4°C. The slides were washed and incubated with secondary biotinylated anti-Rabbit IgG antibody (H+L, Vector Laboratories, Inc.) at 1:500 dilution for 1 hour followed by incubation with avidin-biotin conjugate (1:25 dilution; ABC complex, Vector Laboratories, Inc.) incubation for 30 minutes. The samples were treated with the chromogen diaminobenzidine for antigen detection and the final counterstaining was performed with hematoxylin.

Analysis of myeloid cells populations present in infected tumors

For the characterization of the immune cells within the tumor in response to the virus treatment, B16-F10 melanoma syngeneic model was carried out in C57/BL6J female mice as described before. The animals received a total of three intratumoral injections of PBS or recombinant NDV virus suspension (5×10^6 PFU in 50 μl of PBS), one every 24 hours, and the tumors were isolated 24 hours after the last injection.

For the Immune cell isolation, the tumors were minced, digested with collagenase IV (Roche) for 1 hour at 37*C and passed through 70 um cell strainers in order to obtain single cell suspensions. Cells were layered in a 40% and 90% Percoll gradient (GE Healthcare) and

centrifuged at 1260×g for 40 minutes without brake. The interphase was collected and analyzed by flow cytometry.

Flow Cytometry analysis: Fluorochrome-conjugated antibodies against CD44 (clone IM7) were purchased from BD Pharmingen, against Ly-6C (AL-21) from BD Biosciences, against CD4 (RM4-5), CD8a (53-6.7), CD11b (M1/70), CD11c (N418), CD25 (PC61.5), CD62L (MEL-14) and Foxp3 (FJK-16s) from eBioscience, against CD3 (17A2), CD45 30-F11), CD64 (X54-5/7.1), CD103 (2E7), I-A/I-E (M5/114.15.2) and Ly-6G (1A8) from BioLegend, against CCR2 (475301) from R&D Systems. Cells were incubated with specific antibodies in DPBS containing 0.5% BSA and 2mM EDTA for 20 minutes at 4*C. Intracellular staining for Foxp3 was performed using the transcription factor fixation / permeabilization concentrale and diluent from eBioscience. Samples were acquired on a BD LSRFortessa (Becton Dickinson) using the FACSDiva Software and analyzed with FlowJo software (Tree Star).

Statistical analysis

Statistical significance between results from triplicate samples was determined by 2-tailed Student's *t* test. The results are expressed as mean values ± standard deviations. The comparison of survival curves for the data obtained in the B16-F10 melanoma syngeneic model was performed using the long-rank (Mantel-Cox) test. The analysis of the myeloid cell populations presented within the treated tumors was performed using a 1 way ANOVA (Dunn's Multiple comparison test).

Ethics Statement

All animal procedures performed in this study are in accordance with Institutional Animal Care and Use Committee (IACUC) guidelines, and have been approved by the IACUC of Icahn School of Medicine at Mount Sinai.

Results

Detection of Human Fas receptor expression in rNDV-B1/Fas infected cells

In our study, a new recombinant NDV virus, rNDV-B1/Fas, was generated and assessed for improved oncolytic potential. For this purpose, the ORF of the human Fas receptor was inserted into the backbone of the lentogenic NDV-B1 virus genome between the P and M genes (Fig. 1A) to ensure high level of protein expression during virus replication (1). Insert stability within the viral genome was assessed after six viral growth passages in eggs and the fidelity of its sequence was confirmed by RT-PCR. Comparison of growth properties of rNDV-B1/Fas with those the parental rNDV-B1 in the human cancer cell lines HeLa, A549, HuH-7 and C-33A,as well as in Vero cells showed no differences (Fig. 1B), with both viruses replicating to similar titers and kinetics. Specific expression of Fas receptor after infection with the newly generated virus was detected by immunofluorescence in HeLa cells (Fig. 1C), as well as in other human (A549, HBL, C-33A, Hep2, HuH, PC3) cancer-derived cell lines, and in the African Green monkey cell line Vero (data not shown). As expected, the Fas protein was broadly distributed on the cell surface, where areas of high-density receptor accumulation, could be clearly distinguished (Fig. 1D **upper panel**).

The intracellular localization of the receptor during rNDV-B1/Fas infection was determined by confocal microscopy following immunofluorescent labeling (Fig. 1D **lower panel**). Inside the cell, Fas could be found colocalizing with the early endosome marker Rab5 in the cytoplasmic endosomal compartment, one of the hallmarks of Fas activation. These localization patterns suggest that overexpression of Fas receptor by the recombinant virus results in its activation in the absence of its ligand.

Enhanced cytopathic effect in rNDV-B1/Fas infected-cells correlates with an early activation of the apoptosis response

To determine whether overexpression of Fas receptor during rNDV-B1/Fas virus infection could enhance the inherent pro-apoptotic activity of NDV, we studied specific morphological and biochemical features of this type of cell death. First, apoptosis-specific morphological modifications in rNDV-B1 or rNDV-B1/Fas infected-cells were monitored by microscopy. At 24 hour post-infection, the number of adherent cells was dramatically reduced during rNDV-B1/Fas virus infection as compared to those infected with rNDV-B1. The remaining attached cells presented typical apoptosis morphological landmarks like cytoplasmic membrane blebbing and DNA fragmentation as observed by immunostaining (Fig. 2A). Cells that undergo apoptosis gradually lose metabolic functions leading to cell death. To quantify rNDV-B1/Fas and rNDV-B1 replication-associated cytotoxicity, we performed an MTT viability assay that measures the activity of mitochondrial reductase enzymes which are only active in living cells. rNDV-B1/Fas virus infection resulted in more than 50% reduction in HeLa cells viability at 24 hours post-infection (Fig. 2B, **right panel**). Even at the latest time point of our study, 48 hours post-infection, rNDV-B1 virus did not promote more than 50% reduction in cell viability. Both cytomorphological and viability studies suggest that cells infected with rNDV-B1/Fas undergo an earlier and more potent apoptosis response. This enhanced cytotoxicity was also validated in other human (A549, HuH-7, C-33A) and murine (CT26) cancer-derived cell lines (Figure 2B, **left panel**).

To further characterize the apoptosis response induced by rNDV-B1/Fas infection we performed Annexin-V/PI stains in HeLa infected cells. Since Annexin-V staining precedes PI staining during apoptosis, late stages of apoptosis are characterized by double Annexin-V/PI stain (Fig. 2C). As early as 24 hours post-infection, rNDV-B1/Fas infected cells showed higher number of cells progressing into the final stages of late apoptosis than cells infected with rNDV-B1.

Overexpression of Fas leads to activation of both intrinsic and extrinsic pathways in rNDV-B1/Fas infected cells

We next studied the caspase activation pattern during infection with either rNDV-B1/Fas or rNDV-B1 (Fig. 3A). Protein extracts collected at different time points post-infection were tested to detect active forms of the principal caspases involved in both extrinsic and intrinsic pathways. As compared to rNDV-B1 infected cells extracts, rNDV-B1/Fas infected cells showed activation of caspase 8, 9 and caspase 3 at 24 hours, which is in contrast to their late (48 hours) activation in rNDV-B1 infected cells. This was also accompanied by the presence of cleaved Poly (ADP ribose) polymerase PARP that is a marker for the final stages of programmed cell death.

We next wanted to investigate the contribution of the extrinsic (caspase-8 dependent) pathway into the new modified apoptotic response due to Fas overexpression. Adding specific caspase inhibitors to the post-infection media we could observe that after 24 hours the inhibition of caspase 8 had the strongest effect restricting both caspase 9 and 3 activities in rNDV-B1/Fas infected cells (Fig. 3B). However, caspase 9 inhibition led to a slightly inhibition of caspase 8 and 3 activities. No effects were seen in rNDV-B1 infected cells, since at 24h postinfection there is still no detectable caspase 3, 8 and 9 activation. The apoptosis activation pattern seen in rNDV-B1/Fas-infected cells indicates that the up-regulation of Fas receptor results in co-activation and cooperation in cell death of both the extrinsic (caspase-8 dependent) and intrinsic (caspase-9 dependent) pathways with an important and earlier contribution of the Fas-mediated caspase-8 dependent extrinsic pathway. This cooperative effect is likely responsible for the increase in the general apoptosis response observed during rNDV-B1/Fas infection as compared to rNDV-B1 infection.

rNDV-B1/Fas virus infection leads to interferon response activation and enhances apoptosis induction in murine B16-F10 melanoma cells

Previously to the evaluation of the potential therapeutic effect of the rNDV-B1/Fas virus *in vivo*, we wanted to know if the oncolytic properties displayed by the rNDV-B1/Fas virus in human cancer cell lines *in vitro* would be preserved also in cancer cells of murine origin.

Both, rNDV-B1 and rNDV-B1/Fas viruses were able to replicate at similar levels in B16-F10 showing similar titers and kinetics (Fig. 4B). By confocal microscopy we could observe that the human Fas receptor was highly expressed and broadly distributed on the cell surface as well as in the cytoplasmic endosome compartment of the murine cell line (Fig. 4A), same way as we described before for the human cancer cell line HeLa (Fig. 1C and D). rNDV-B1/Fas virus exerted higher and earlier cytotoxicity in the murine cancer cell line (Fig. 4C) and this cytotoxicity was also correlated with an earlier activation of the apoptosis response, with the presence of active forms of caspase 3 detected 24 hours post-infection (Fig. 4D).

Since the NDV therapeutic effect *in vivo* involves an active interferon response induction upon virus infection (5), we wanted to evaluate the potential stimulation of the rNDV-B1/Fas virus in the murine B16-F10 melanoma cells. To assess this question, B16-F10 cells with rNDV-B1 or rNDV-B1/Fas viruses at a MOI of 1 and total RNA was isolated 8 hours post-infection. Immortalized NIH/3T3 murine fibroblasts were infected in similar conditions to be used as a positive control. The levels of INF-beta mRNA as well as those for the interferon stimulated genes (ISGs) IFT1, IRF7 and OAS1 were evaluated by qPCR (Fig. 4E). No difference was found between the viruses and the B16-F10 cells shown similar levels of interferon induction as the immortalized fibroblasts, 8 hours upon infection.

Intratumoral treatment with rNDV-B1/Fas virus enhances survival, promotes complete tumor remission and protection against re-challenge in melanoma syngeneic murine model

To assess whether the improvement of the pro-apoptotic activity of rNDV-B1/Fas would enhance the inherent oncolytic properties of NDV *in vivo*, we tested its anti-tumor capacity

in melanoma syngeneic tumor models. Murine melanoma B16-F10 cells were subcutaneously implanted in the leg flanks of C57BL/6 mice. Tumors were allowed to develop until palpable and a total of three intratumoral injections of each virus or PBS were administrated, as described in Materials and Methods. Treatment with rNDV-B1/Fas virus restricted tumor progression (Fig. 4F), leading to a significant improvement in survival compared to mice treated with rNDV-B1 or PBS. rNDV-B1 treatment delayed tumor growth, but only resulted in complete tumor remission in 12% of treated animals. However, complete tumor remission was observed in 83% of mice treated with rNDV-B1/Fas (Fig. 4F). These remaining tumor-free animals did not show tumor recurrence, loss of weight or any other sign of sickness.

We also wanted to know if the enhancement of the apoptotic response could also influence the emergence of a long time protection against cancer relapse. To assess this question, a new set of animals were used to induce a syngeneic melanoma model and once they presented tumors, the animals were subjected to the same treatment conditions described before. The rNDV-B1/Fas virus treatment induced an overall enhancement of survival of 43% and complete tumor revision was also reported within the experimental group (Fig. 4G). However, in this study, none of the animals treated with the wild type virus underwent tumor remission. The survivors treated by the rNDV-B1/Fas virus that demonstrated complete recovery for up to 30 days, were then re-challenged against melanoma by subcutaneous re-injection of B16-F10 melanoma cells in the flank of the opposite leg. Those animals, as a part of a long-term study, were under periodical observation and no sign of tumor reversion or any other sign of sickness was reported for up to 6 months.

Early and enhanced apoptosis response during rNDV-B1/Fas virotherapy could be a key point for a more specific immune response against the tumor

We wanted to know if the earlier pro-apoptotic activity exerted by rNDV-B1/Fas virus *in vitro* could be also a main feature of the rNDV-B1/Fas treated tumors *in vivo*. For that propose, murine melanoma B16-F10 cells were intradermally implanted on the flank of the leg in C57BL/6 mice. After 10 days the generated tumors were intratumorally treated with a single dose of PBS or virus suspension. At. 24 hours post-inoculation, the mice were culled and the tumors were removed and processed for general histopathology analysis, virus immunodetection and apoptosis markers determination (Fig 5A, B, C and Supplementary Fig. S1 A and B). At this time point (24h post treatment), tumor histopathology analysis did not show any relevant differences in markers of advanced melanoma progression, such as high vascularization and necrosis, between treatment groups (PBS, rNDV-B1 or rNDV-B1/Fas treated tumors), as monitored after hematoxylin and eosin staining (Fig. 5A). Only rNDV-B1 or rNDV-B1/Fas infected tumors were positive for anti-NDV F protein detection (Fig. 5B) but there were no significant differences related to infection distribution or virus spread between these two groups. However, we could detect a notable presence of active caspase 3 positive cells in rNDV-B1/Fas treated samples compared to both PBS and wild-type virus treatments (Fig. 5C). This indicates that the earlier and improved apoptosis response previously described *in vitro* for rNDV-B1/Fas (Fig. 2, 3 and 4) also occurs after intratumoral inoculation *in vivo* (Fig. 4A and B).

Last, we wanted to refine the characterization of the therapeutic effect exerted by the recombinant rNDV-B1/Fas in the early phase of the treatment by analyzing the innate immune cells populations resident within the tumors upon virus treatment. For that propose, we carried out a new syngeneic melanoma assay in C57BL/6 mice, following the same proceedings previously described. In this particular experiment, the animals received the complete treatment (3 doses of PBS or recombinant virus injected intratumorally and were culled 24 hours after the administration of the last dose.

The tumors were removed and specifically processed for the isolation and analysis by Flow cytometry of the different myeloid cells lineages, as is mentioned in Material and Methods. As expected, the response to both viruses demonstrated been more immunogenic compared with the PBS treatment, with a decrease in Dendritic cells and an increase in pro-inflammatory Macrophages and Neutrophils resident at that moment in the infected tumors (Fig. 5D). Further investigations would be needed it to evaluate the contribution of the innate immune response in our model. An improved and more specific innate immune response due a better immunological cell death of the tumor cells would be the major determinant in the long term protection observed in the rNDV-B1/Fas treated mice

Discussion

During the last decade, new studies exploring Newcastle disease virus antitumor characteristics have emerged and a new generation of recombinant NDVs has been engineered attempting to enhance its natural oncolytic capacity (4). In our current study, to design an improved therapeutic agent, we attempted to increase cell death induced in NDV-infected tumors. To do so, we generated a recombinant NDV encoding the human tumor necrosis factor receptor Fas (TNFRSF6, CD95). Neither Fas nor its ligand Fas-L had come out in the list of host elements involved in the NDV-stimulated apoptosis response. Our rationale in designing such vector is that overexpression of Fas receptor in infected cells would lead to the activation of the extrinsic apoptosis pathway which would both complement and increase the pro-apoptotic capacity of NDV otherwise mainly mediated by the activation of the intrinsic pathway (30–32). This may enhance the anti-tumor activity of NDV in several ways, first enhancing tumor cell death during direct infection, second, increasing immune mediated cell death of infected cells, and third, promoting the release of pro-inflammatory mediators that promote immune activation of anti-tumor responses.

At this moment we do not know which of these factors or combination of factors is the main driver in the increased therapeutic effect of rNDV-B1/Fas.

Our *in vitro* studies with rNDV-B1/Fas demonstrated high levels of the recombinant human Fas receptor expression in different human and mouse infected cancer cell lines. Fas receptor expressed by NDV exhibited widespread distribution throughout the cell membrane with areas of receptor aggregates, consistent with Fas receptor activation by overexpression. The recruitment and stabilization of pre-assembled receptors in signaling protein oligomerization structures (SPOTS) in the cytoplasmic membrane are necessary to initiate signal transduction. This is physiologically mediated through Fas/FasL interaction (40). However, during rNDV-B1/Fas infection the overexpressed receptor was able to form these

pro-apoptotic SPOTS in the cytoplasmic membrane in absence of FasL stimulus. A similar phenomenon was previously described in other approaches in which the main aim was to increase or stabilize the receptor at the membrane surface (41–45). Also, we could detect the presence of Fas receptor in the cytoplasmic endosomal compartment, previously described to be a secondary and necessary location for the amplification of caspase mediated signaling (46). These results support that in rNDV-B1/Fas infected cells the required environment and cellular compartmentalization necessary for Fas receptor activity has been achieved by overexpression in a ligand independent-manner.

Furthermore, the rNDV-B1/Fas-infected cells display a different caspase activation profile than the one in rNDV-B1-infected cells. According to previous studies, wild type NDV-infected cells undergo apoptotic cell death at a late step during virus replication through the activation of both the intrinsic and extrinsic apoptosis pathways (20–23). We confirmed this by assessing the presence of caspase 9, caspase 8 and caspase 3 48 hours post-infection in rNDV-B1-infected cells. In contrast, after rNDV-B1/Fas infection we detected the presence of the active forms of the extrinsic pathway initiator caspase 8 and the executor caspase 3 earlier on during infection. To our knowledge, no other tested strain of NDV has shown a similar apoptosis induction profile, with only one report of a velogenic strain inducing an early activation of the extrinsic pathway (47), which preceded the standard intrinsic activation and was apparently independent of it. Interestingly and in blatant contrast, during rNDV-B1/Fas infection the presence of active forms of the intrinsic pathway initiator caspase 9 was detected at the same time as caspase 8 and caspase 3, which suggest the possibility of an early co-activation of both pathways. The interdependence between pathways was assessed by inhibition of the activity of the principal initiators caspase 8 and caspase 9. We observed that the down-regulation of caspase 8 activity strongly repressed not only the execution phase caspase 3-dependent but also caspase 9 activity which suggests that in rNDV-B1/Fas infected cells the strongest pro-apoptotic stimuli comes from the extrinsic signaling pathway. Taking under consideration the previously known elements involved in NDV-mediated apoptosis, we propose that overexpression of Fas receptor during rNDV-B1/Fas infection acts as an early apoptotic trigger that promotes up-regulation of the extrinsic pathway and increased levels of cell death.

In our *in vivo* studies, we tested the oncolytic activity of rNDV-B1/Fas and rNDV-B1 against B16 melanoma, one of the more aggressive syngeneic murine tumor models. rNDV-B1/Fas virotherapy demonstrated an extraordinary efficacy, not only improving survival time but also inducing complete tumor remission and long term protection against tumor relapse. A single dose of the virus suspension was enough to unleash a strong apoptosis response in tumor cells perceptible as early as 24 hours post virus administration. Supported by our *in vitro* observations, the *in vivo* results strongly suggest that an early and enhanced apoptosis response might play a key role in the rNDV-B1/Fas successful virotherapy. This enrichment in apoptotic cell death within the tumor in early stages during the treatment and the consequent modification of the tumor microenvironment could be boosting a better and more specific innate immune response against the tumor and therefore provide the perfect scenario to the emergence of a long term adaptive immune response.

An improvement in survival and complete tumor remission were also achieved by rNDV-B1/Fas treatment of colon carcinoma syngeneic murine tumor model (data not shown). Melanoma and colon carcinoma are some of the human cancers with the worst prognosis due to their metastatic capacity and resistance to chemotherapeutic drugs in which defects on the Fas/FasL system are known to be responsible for the tumor progression (35, 48, 49). The list of malignant tumors in which Fas/FasL deficits have been implicated also includes pancreatic, thyroid and lung carcinomas, breast and ovarian cancer, and blood cancers, among others (35, 50). Our results obtained in the murine model open the possibility of a new approach for the treatment of such aggressive tumors, providing a local therapy that combines the specificity of viral infection of cancer cells and the enhancement of the pro-apoptotic capacity of NDV.

Supplementary Material

Refer to Web version on PubMed Central for supplementary material.

Acknowledgements

We are grateful to Faustino Mollinedo and Consuelo Gajate (CIC, Salamanca, Spain) for providing pL430-Fas plasmid. Martin Perez-Andres (Assistant professor, Dept. Medicine, Serv. Cytometry, CIC-Universidad de Salamanca) for his cooperation. We thank Richard Cadagan and Osman Lizardo for excellent technical assistance. Confocal laser scanning microscopy was performed at the Icahn School of Medicine at Mount Sinai-Microscopy Shared Resource Facility.

Financial Suport:

R01AI088770 from NIAID to A. García-Sastre and PI08/1813 from the Spanish Fondo de Investigaciones Sanitarias (co-financed by FEDER funds from the EU) to E.Villar. S.Cuadrado-Castano was a predoctoral fellowship holder from the Spanish JCYL (co-financed by European Social Funds (EDU/330/2008; 2008–2012). M. Mansour was supported by NCI 5 T32 CA 78207-13 training grant.

References

1. Parks, GD.; Lamb, RA. Paramyxoviridae: The viruses and Their replication. In: Fields, BN.; Knipe, DM.; Howley, PM., editors. Fields virology. Fifth ed.. Philadelphia: Wolters Kluwer Health/ Lippincott Williams & Wilkins; 2007. p. 48
2. Cassel WA, Garrett RE. Newcastle Disease Virus as an Antineoplastic Agent. Cancer. 1965; 18:863–868. [PubMed: 14308233]
3. Sinkovics JG, Horvath JC. Newcastle disease virus (NDV): brief history of its oncolytic strains. J Clin Virol. 2000; 16:1–15. [PubMed: 10680736]
4. Zamarin D, Palese P. Oncolytic Newcastle disease virus for cancer therapy: old challenges and new directions. Future Microbiol. 2012; 7:347–367. [PubMed: 22393889]
5. Zamarin D, Holmgaard RB, Subudhi SK, Park JS, Mansour M, Palese P, et al. Localized oncolytic virotherapy overcomes systemic tumor resistance to immune checkpoint blockade immunotherapy. Science translational medicine. 2014; 6:226ra32.
6. Lam HY, Yeap SK, Rasoli M, Omar AR, Yusoff K, Suraini AA, et al. Safety and clinical usage of newcastle disease virus in cancer therapy. Journal of biomedicine & biotechnology. 2011; 2011:718710. [PubMed: 22131816]
7. Peeters BP, de Leeuw OS, Koch G, Gielkens AL. Rescue of Newcastle disease virus from cloned cDNA: evidence that cleavability of the fusion protein is a major determinant for virulence. Journal of virology. 1999; 73:5001–5009. [PubMed: 10233962]
8. Nakaya T, Cros J, Park MS, Nakaya Y, Zheng H, Sagrera A, et al. Recombinant Newcastle disease virus as a vaccine vector. Journal of virology. 2001; 75:11868–11873. [PubMed: 11689668]

9. Vigil A, Park MS, Martinez O, Chua MA, Xiao S, Cros JF, et al. Use of reverse genetics to enhance the oncolytic properties of Newcastle disease virus. Cancer research. 2007; 67:8285–8292. [PubMed: 17804743]
10. Zhao H, Janke M, Fournier P, Schirrmacher V. Recombinant Newcastle disease virus expressing human interleukin-2 serves as a potential candidate for tumor therapy. Virus Res. 2008; 136:75–80. [PubMed: 18538434]
11. Vigil A, Martinez O, Chua MA, Garcia-Sastre A. Recombinant Newcastle disease virus as a vaccine vector for cancer therapy. Molecular therapy : the journal of the American Society of Gene Therapy. 2008; 16:1883–1890. [PubMed: 18714310]
12. Zamarin D, Vigil A, Kelly K, Garcia-Sastre A, Fong Y. Genetically engineered Newcastle disease virus for malignant melanoma therapy. Gene Ther. 2009; 16:796–804. [PubMed: 19242529]
13. Puhler F, Willuda J, Puhlmann J, Mumberg D, Romer-Oberdorfer A, Beier R. Generation of a recombinant oncolytic Newcastle disease virus and expression of a full IgG antibody from two transgenes. Gene Ther. 2008; 15:371–383. [PubMed: 18200068]
14. Galluzzi L, Vitale I, Abrams JM, Alnemri ES, Baehrecke EH, Blagosklonny MV, et al. Molecular definitions of cell death subroutines: recommendations of the Nomenclature Committee on Cell Death 2012. Cell Death Differ. 2012; 19:107–120. [PubMed: 21760595]
15. Elmore S. Apoptosis: a review of programmed cell death. Toxicol Pathol. 2007; 35:495–516. [PubMed: 17562483]
16. Igney FH, Krammer PH. Death and anti-death: tumour resistance to apoptosis. Nature reviews Cancer. 2002; 2:277–288.
17. Kerr JF, Winterford CM, Harmon BV. Apoptosis. Its significance in cancer and cancer therapy. Cancer. 1994; 73:2013–2026. [PubMed: 8156506]
18. Johnstone RW, Ruefli AA, Lowe SW. Apoptosis: a link between cancer genetics and chemotherapy. Cell. 2002; 108:153–164. [PubMed: 11832206]
19. Kaufmann SH, Vaux DL. Alterations in the apoptotic machinery and their potential role in anticancer drug resistance. Oncogene. 2003; 22:7414–7430. [PubMed: 14576849]
20. Fabian Z, Csatary CM, Szeberenyi J, Csatary LK. p53-independent endoplasmic reticulum stress-mediated cytotoxicity of a Newcastle disease virus strain in tumor cell lines. Journal of virology. 2007; 81:2817–2830. [PubMed: 17215292]
21. Elankumaran S, Rockemann D, Samal SK. Newcastle disease virus exerts oncolysis by both intrinsic and extrinsic caspase-dependent pathways of cell death. Journal of virology. 2006; 80:7522–7534. [PubMed: 16840332]
22. Ravindra PV, Tiwari AK, Ratta B, Chaturvedi U, Palia SK, Chauhan RS. Newcastle disease virus-induced cytopathic effect in infected cells is caused by apoptosis. Virus Res. 2009; 141:13–20. [PubMed: 19152817]
23. Mansour M, Palese P, Zamarin D. Oncolytic specificity of Newcastle disease virus is mediated by selectivity for apoptosis-resistant cells. J Virol. 2011; 85:6015–6023. [PubMed: 21471241]
24. Locksley RM, Killeen N, Lenardo MJ. The TNF and TNF receptor superfamilies: integrating mammalian biology. Cell. 2001; 104:487–501. [PubMed: 11239407]
25. Trauth BC, Klas C, Peters AM, Matzku S, Moller P, Falk W, et al. Monoclonal antibody-mediated tumor regression by induction of apoptosis. Science. 1989; 245:301–305. [PubMed: 2787530]
26. Nagata S, Golstein P. The Fas death factor. Science. 1995; 267:1449–1456. [PubMed: 7533326]
27. Yonehara S, Ishii A, Yonehara M. A cell-killing monoclonal antibody (anti-Fas) to a cell surface antigen co-downregulated with the receptor of tumor necrosis factor. J Exp Med. 1989; 169:1747–1756. [PubMed: 2469768]
28. Siegel RM, Chan FK, Chun HJ, Lenardo MJ. The multifaceted role of Fas signaling in immune cell homeostasis and autoimmunity. Nat Immunol. 2000; 1:469–474. [PubMed: 11101867]
29. Schneider P, Bodmer JL, Holler N, Mattmann C, Scuderi P, Terskikh A, et al. Characterization of Fas (Apo-1, CD95)-Fas ligand interaction. The Journal of biological chemistry. 1997; 272:18827–18833. [PubMed: 9228058]
30. Schutze S, Tchikov V, Schneider-Brachert W. Regulation of TNFR1 and CD95 signalling by receptor compartmentalization. Nat Rev Mol Cell Biol. 2008; 9:655–662. [PubMed: 18545270]

31. Zhao Y, Sui X, Ren H. From procaspase-8 to caspase-8: revisiting structural functions of caspase-8. J Cell Physiol. 2010; 225:316–320. [PubMed: 20568107]
32. Scaffidi C, Fulda S, Srinivasan A, Friesen C, Li F, Tomaselli KJ, et al. Two CD95 (APO-1/Fas) signaling pathways. Embo J. 1998; 17:1675–1687. [PubMed: 9501089]
33. Takahashi T, Tanaka M, Inazawa J, Abe T, Suda T, Nagata S. Human Fas ligand: gene structure, chromosomal location and species specificity. International immunology. 1994; 6:1567–1574. [PubMed: 7826947]
34. Pardo J, Bosque A, Brehm R, Wallich R, Naval J, Mullbacher A, et al. Apoptotic pathways are selectively activated by granzyme A and/or granzyme B in CTL-mediated target cell lysis. The Journal of cell biology. 2004; 167:457–468. [PubMed: 15534000]
35. Muschen M, Warskulat U, Beckmann MW. Defining CD95 as a tumor suppressor gene. J Mol Med (Berl). 2000; 78:312–325. [PubMed: 11001528]
36. Debatin KM, Krammer PH. Death receptors in chemotherapy and cancer. Oncogene. 2004; 23:2950–2966. [PubMed: 15077156]
37. Israelow B, Narbus CM, Sourisseau M, Evans MJ. HepG2 cells mount an effective antiviral interferon-lambda based innate immune response to hepatitis C virus infection. Hepatology. 2014; 60:1170–1179. [PubMed: 24833036]
38. Park MS, Garcia-Sastre A, Cros JF, Basler CF, Palese P. Newcastle disease virus V protein is a determinant of host range restriction. Journal of virology. 2003; 77:9522–9532. [PubMed: 12915566]
39. Livak KJST. Analysis of relative gene expression data using real-time quantitative PCR and the 2(-Delta Delta C(T)) method. Methods. 2001; 25:402–408. [PubMed: 11846609]
40. Siegel RM, Muppidi JR, Sarker M, Lobito A, Jen M, Martin D, et al. SPOTS: signaling protein oligomeric transduction structures are early mediators of death receptor-induced apoptosis at the plasma membrane. J Cell Biol. 2004; 167:735–744. [PubMed: 15557123]
41. Shinoura N, Ohashi M, Yoshida Y, Kirino T, Asai A, Hashimoto M, et al. Adenovirus-mediated overexpression of Fas induces apoptosis of gliomas. Cancer Gene Ther. 2000; 7:224–232. [PubMed: 10770630]
42. Gajate C, Mollinedo F. Lipid rafts and Fas/CD95 signaling in cancer chemotherapy. Recent patents on anti-cancer drug discovery. 2011; 6:274–283. [PubMed: 21762074]
43. Zhuang S, Kochevar IE. Ultraviolet A radiation induces rapid apoptosis of human leukemia cells by Fas ligand-independent activation of the Fas death pathways. Photochem Photobiol. 2003; 78:61–67. [PubMed: 12929750]
44. Delmas D, Rebe C, Lacour S, Filomenko R, Athias A, Gambert P, et al. Resveratrol-induced apoptosis is associated with Fas redistribution in the rafts and the formation of a death-inducing signaling complex in colon cancer cells. The Journal of biological chemistry. 2003; 278:41482–41490. [PubMed: 12902349]
45. Legembre P, Beneteau M, Daburon S, Moreau JF, Taupin JL. Cutting edge: SDS-stable Fas microaggregates: an early event of Fas activation occurring with agonistic anti-Fas antibody but not with Fas ligand. J Immunol. 2003; 171:5659–5662. [PubMed: 14634070]
46. Lee KH, Feig C, Tchikov V, Schickel R, Hallas C, Schutze S, et al. The role of receptor internalization in CD95 signaling. The EMBO journal. 2006; 25:1009–1023. [PubMed: 16498403]
47. Ravindra PV, Tiwari AK, Ratta B, Bais MV, Chaturvedi U, Palia SK, et al. Time course of Newcastle disease virus-induced apoptotic pathways. Virus Res. 2009; 144:350–354. [PubMed: 19501124]
48. Shimizu M, Yoshimoto T, Sato M, Matsuzawa A, Takeda Y. Frequency and resistance of CD95 (Fas/Apo-1) gene-transfected tumor cells to CD95-mediated apoptosis by the elimination and methylation of integrated DNA. Int J Cancer. 2006; 119:585–592. [PubMed: 16506211]
49. Soengas MS, Lowe SW. Apoptosis and melanoma chemoresistance. Oncogene. 2003; 22:3138–3151. [PubMed: 12789290]
50. Caldwell SA, Ryan MH, McDuffie E, Abrams SI. The Fas/Fas ligand pathway is important for optimal tumor regression in a mouse model of CTL adoptive immunotherapy of experimental CMS4 lung metastases. J Immunol. 2003; 171:2402–2412. [PubMed: 12928387]

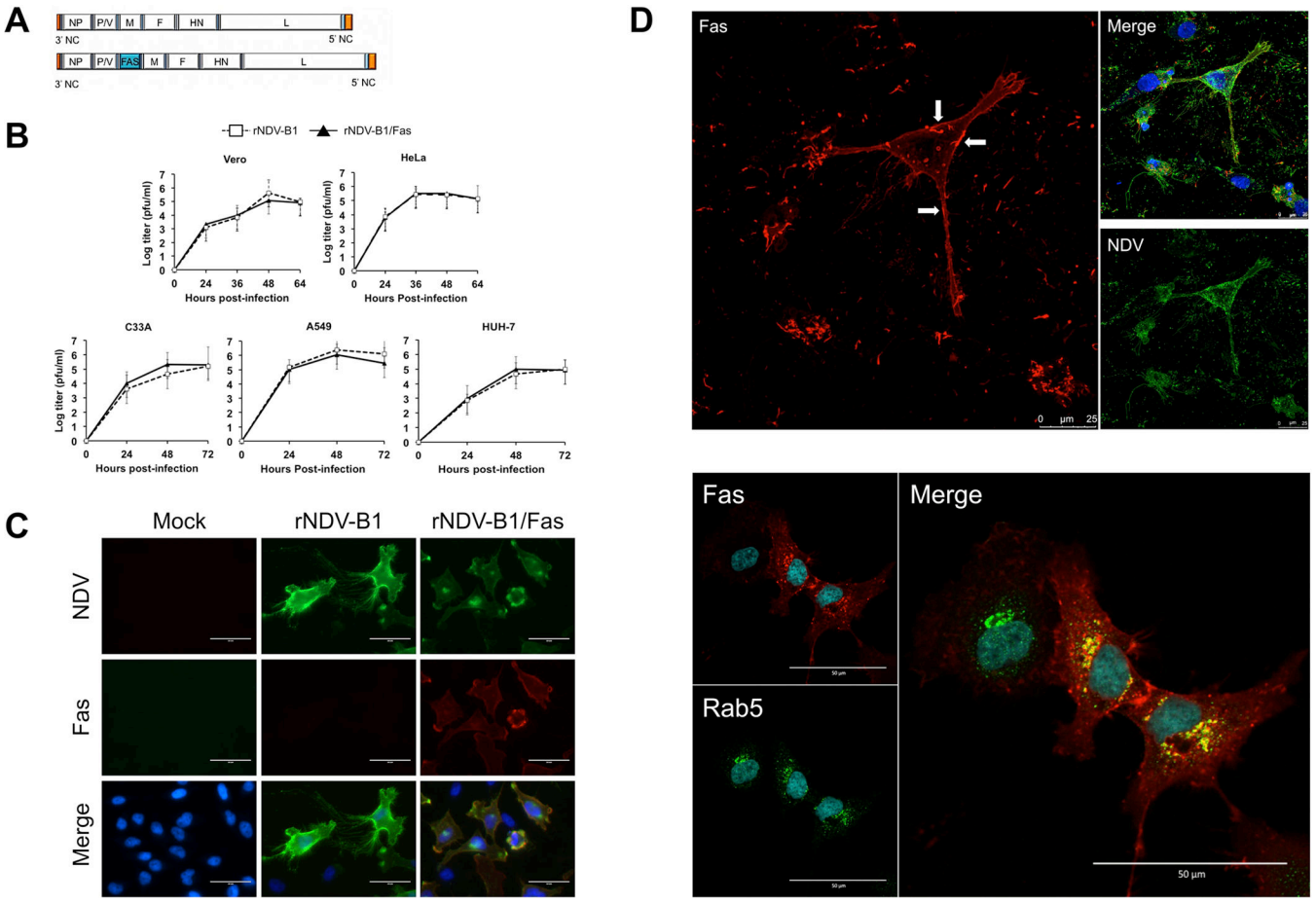

Figure 1. Generation and characterization of recombinant rNDV-B1/Fas

A, schematic representation of the genomes of rNDV-B1 and rNDV-B1/Fas, showing the position between the P/V and M genes in which the new ORF was inserted. **B, multicycle growth curves of rNDV-B1 and rNDV-B1/Fas**. HeLa, A549, HuH-7, C-33A and Vero cells monolayers were infected at an MOI of 0.01 PFU/cell. At different time-points post-infection viral titers in the supernatant were determined. Data points show mean values from three replicates with error bars representing standard deviations. **C, immunofluorescence detection of the expression of human Fas receptor in rNDV-B1/Fas-infected cells**. HeLa cells were infected at an MOI of 1 PFU/cell, fixed 24 hours post-infection and stained with a monoclonal antibody against human Fas (red), polyclonal serum against NDV (green) and Hoechst for nuclear contrast (blue). Scale bar 50µm. **D, cellular distribution of recombinant Fas receptor upon rNDV-B1/Fas infection**. Cells were infected at an MOI of 1 PFU/cell, fixed 20 hours post-infection and stained with monoclonal anti-human Fas antibody (red), polyclonal serum anti NDV (green, upper panel) or antibody against the early endosome marker rab5 (green, lower panel) and Hoechst for nuclear contrast. Upper panel: cytoplasmic membrane location of Fas receptor. Main upper panel: white arrows pointing at higher density receptor areas at the membrane surface. Scale bar 25µm. Lower panel: Fas receptor endosomal compartment location. Main lower panel: co-localization of human Fas receptor and Rab5 into endosomal compartment. Scale bar 50µm.

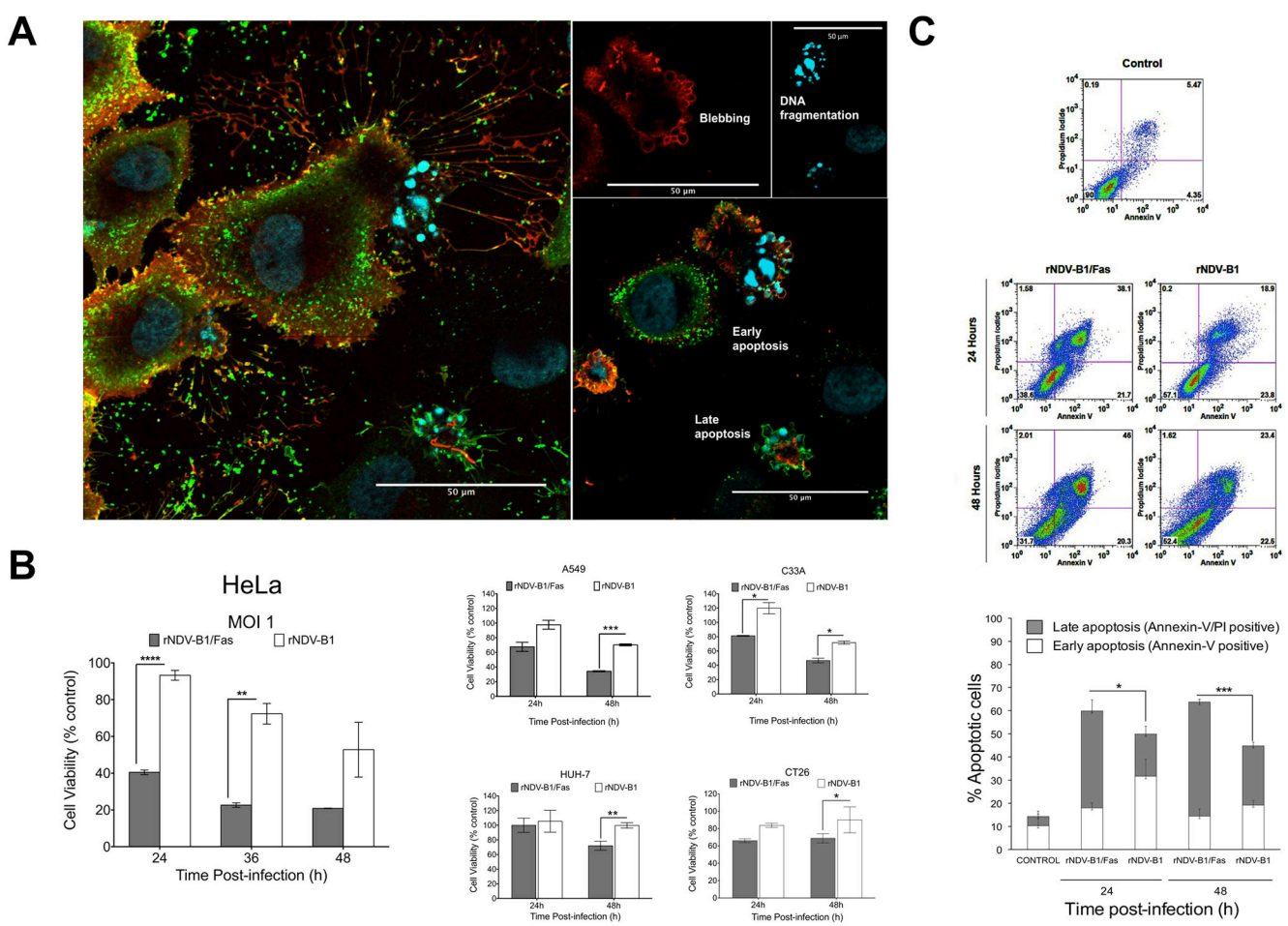

Figure 2. rNDV-B1/Fas infection induces higher cytotoxicity and an earlier apoptotic response in cancer cells

A, cytopathic effect due to rNDV-B1/Fas infection. Confocal microscopy images of HeLa cells infected with rNDV-B1/Fas. Cells were infected at an MOI of 1 PFU/cell, fixed 20 hours post-infection and stained with monoclonal anti-human Fas antibody (red), polyclonal anti-NDV serum (green) and Hoechst for nuclear contrast. Left panel: composite Z-stack of six optical slices showing membrane and intracellular distribution of Fas receptor. Left panels show different late apoptotic feautures, like membrane blebbing and DNA fragmentation, observed among the infected population. Scale bar 50µm. **B, cytotoxicity**. HeLa, A549, HUH-7, C-33A and Ct26 cells were infected at an MOI of 1 PFU/cell and their viability was determined by MTT viability assay at different time points (24, 36 and 48 hours post-infection) (n=3, *p<0.05 **p<0.005, ***p< 0.0005).**C, apoptosis induction during rNDV-B1 and rNDV-B1/Fas infection**. HeLa cells were infected at an MOI of 1 PFU/cell, collected at different times post-infection and double stained with Annexin-V/PI. Early (Annexin-V-positive) and late (Annexin-V/PI-double positive) apoptotic populations were assessed by flow cytometric analysis. Internal axes were defined using Annexin-V/PI data from mock uninfected HeLa cells. Density plots from one out of three independent experiments are shown. The percentage distribution of the different apoptotic stages is also shown (n=3; *p<0.05, ***p<0.0005).

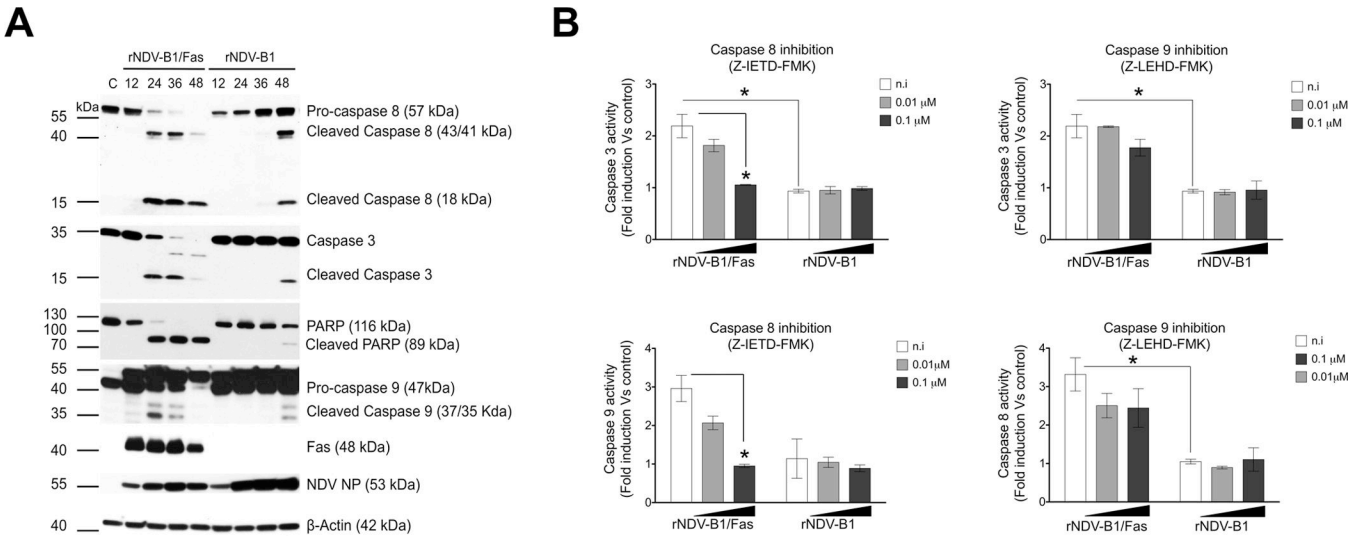

Figure 3. rNDV-B1/Fas infected cells display a modified NDV-induced apoptotic response

A, time course of caspase activation during rNDV-B1/Fas and rNDV-B1 viruses infection. Western blot. HeLa cells were infected with rNDV-B1/Fas and rNDV-B1 at an MOI of 1 PFU/cell and lysates were obtained at different time points post-infection. Differential caspase activation pattern was assessed by western blot using specific anti-caspase 8, 3, 9 and PARP antibodies. Fas receptor expression was detected using an anti-human Fas monoclonal antibody. Viral replication (NP levels) was detected using an anti-NDV polyclonal serum.

B, extrinsic and intrinsic pathways interdependence. HeLa cells were infected with rNDV-B1/Fas and rNDV-B1 at an MOI of 1 PFU/cell and different amount of specific caspase 8 (Z-IETD-FMK) or caspase 9 (Z-LEHD-FMK) inhibitors were added to the post-infection media. After 24 hours post-infection, caspase 8, caspase 9 and caspase 3 activities were evaluated using a luciferase-based caspase activity reporter assay (n=3; *p<0.05).

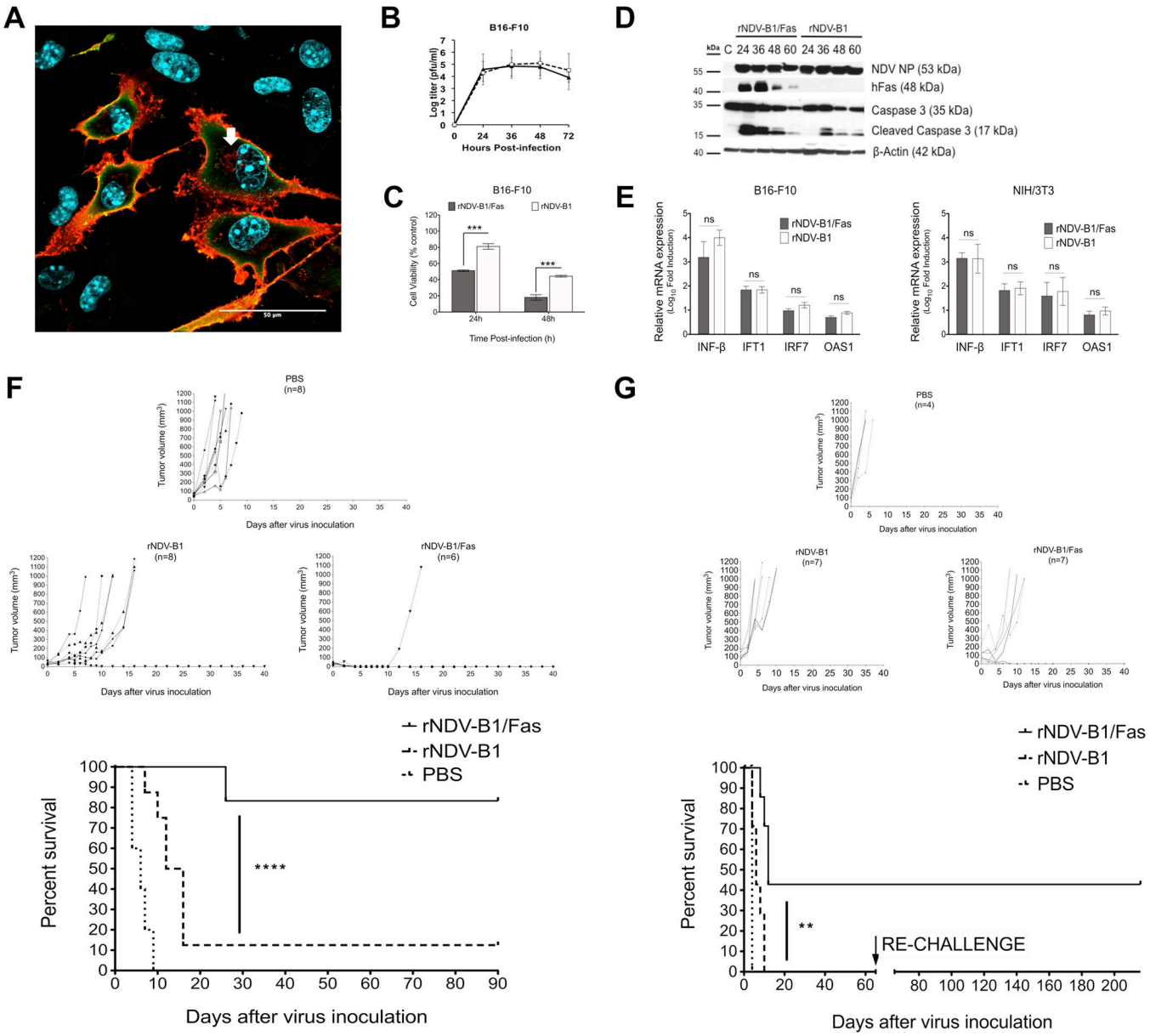

Figure 4. rNDV-B1/Fas virus exerts higher oncolytic capacity and increases survival in a syngeneic melanoma murine model

A, immunofluorescence detection of human Fas receptor in rNDV-B1/Fas-B16-F10 infected cells. Confocal microscopy image of murine melanoma B16-F10 cells infected with rNDV-B1/Fas. Cells were infected at an MOI of 1 PFU/cell, fixed 20 hours post-infection and stained with monoclonal anti-human Fas antibody (red), polyclonal anti-NDV serum (green) and Hoechst for nuclear contrast. Scale bar 50μm. White arrow points endosome compartment localization of the recombinant human Fas receptor. **B, multicycle growth curves**. B16-F10 monolayers were infected at an MOI of 0.01 PFU/cell. At different time-points post-infection viral titers in the supernatant were determined. Data points show mean values from three replicates with error bars representing standard deviations. **C, cytotoxicity**. B16-F10cells were infected at an MOI of 1 PFU/cell and their viability was

determined by MTT viability assay at different time points (24, 36 and 48 hours post-infection) (n=3, ***p< 0.0005). **D, time course of caspases activation. Western blot**. B16-F10 cells were infected with rNDV-B1/Fas and rNDV-B1 at an MOI of 1 PFU/cell and lysates were obtained at different time points post-infection. Apoptosis activation was assessed by western blot using an specific anti-caspase 3 antibody. Human Fas receptor expression was detected using an anti-human Fas monoclonal antibody. Viral replication (NP levels) was detected using an anti-NDV polyclonal serum. **E, Interferon response induction in infected cells**. Monolayers of B16-F10 and NIH/373 cells were infected with the virus suspension at an MOI of 1 PFU/cell.

Total RNAs from cultured cells were isolated 8 hours post-infection. Mean n-Log_{10} fold expression levels of cDNA from three individual biological samples, each measured in triplicate, were normalized to 18S rRNA levels and calibrated to mock-treated samples. mRNA expression levels for INF-beta, IFT1, IFR7 and OAS1 were evaluated in both cell lines (ns> 0.05). **F, oncolytic capacity of rNDV-B1/Fas and rNDV-B1 viruses in syngeneic murine melanoma tumor model. Tumor growth curves and long term survival report**. B16-F10 cells were implanted in the flank of the posterior right leg of C57BL/6 mice. Starting on day ten after tumor cell line injection, the animals were intratumoral treated every other day with a total of three doses of 5×10^6 PFU of rNDV-B1/Fas, rNDV-B1 or PBS for control mice. Tumor volume was monitored every 48 hours or every 24 hours when approaching the experimental end point of 1000 mm^3, after which mice were euthanized (****p< 0.0001). **G, long term survival and protection against melanoma re-challenge**. Syngeneic melanoma tumors and treatment were performed as described in F. After 30 days of absence of tumor, B16-F10 cells were re-implanted in the flank of the opposite leg. The new development or relapse of tumors was reviewed periodically up to 6 months.

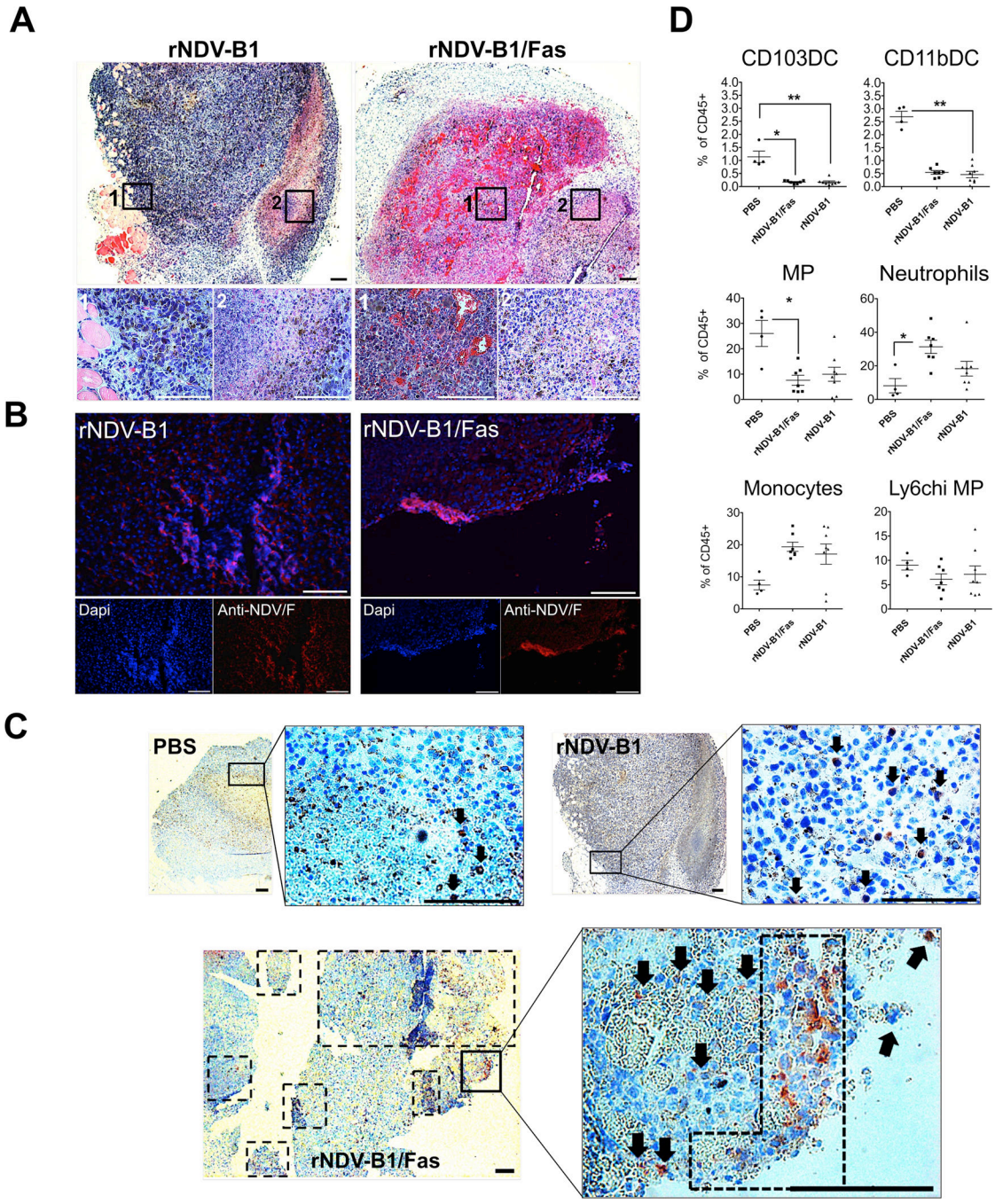

Figure 5. rNDV-B1/Fas intratumoral treatment leads to earlier and enhanced apoptotic response and differential immune infiltration *in vivo*

A, histopathology. Hematoxylin and eosin staining of 5 μm-thick sections from rNDV-B1 or rNDV-B1/Fas treated tumors. White squares note magnified areas corresponding with 1 and 2 lower panels. Black scale bar: 200 μm. White scale bar: 100 μm. **B, virus immunodetection**. Microscopy images of tumor treated samples showing virus infection 24 hours after intratumoral administration. 5 μm-thick sections from rNDV-B1 or rNDV-B1/Fas treated tumors were stained with monoclonal anti-NDV F protein (red) and Dapi

(blue) for nuclear contrast. White square note magnified area. White scale bar: 100 μm. **C, apoptosis detection in fixed tumor samples**. Active caspase 3 immunodetection in tumor-treated samples 24 hours post-injection. 5 μm-thick sections from PBS, rNDV-B1 or rNDV-B1/Fas tumor-treated samples were stained with polyclonal anti-active caspase 3 protein (red) and hematoxilin (blue) for counterstaining. Black squares note magnified areas. Black arrows and dot square note caspase 3 positive cells. Scale bar 200 μm. **D. Analysis of myeloid populations within the tumor microenvironment**. B16-F10 cells were implanted in the flank of the posterior right leg of C57BL/6 mice. Starting on day ten after tumor cell line injection, the animals were intratumorally treated every 24 hours with a total of three doses of 5×10^6 PFU of rNDV-B1/Fas, rNDV-B1 or PBS for control mice. 24 hours after the last dose, the tumors were removed and specifically processed for the isolation and analysis by Flow cytometry of the different myeloid cells lineages. Values for each of the populations were expressed as a percentage respect to the total CD45 positive cells isolated from each tumor (*p< 0.05, **p, 0.005).